REPORT

Homozygosity Mapping Reveals *PDE6C* Mutations in Patients with Early-Onset Cone Photoreceptor Disorders

Alberta A.H.J. Thiadens,[1,2] Anneke I. den Hollander,[3,4] Susanne Roosing,[2] Sander B. Nabuurs,[4,5] Renate C. Zekveld-Vroon,[1] Rob W.J. Collin,[2,3,4] Elfride De Baere,[6] Robert K. Koenekoop,[7] Mary J. van Schooneveld,[8] Tim M. Strom,[9] Janneke J.C. van Lith-Verhoeven,[3] Andrew J. Lotery,[10] Norka van Moll-Ramirez,[11] Bart P. Leroy,[6,12] L. Ingeborgh van den Born,[13] Carel B. Hoyng,[3] Frans P.M. Cremers,[2,4,*] and Caroline C.W. Klaver[1,14]

Cone photoreceptor disorders form a clinical spectrum of diseases that include progressive cone dystrophy (CD) and complete and incomplete achromatopsia (ACHM). The underlying disease mechanisms of autosomal recessive (ar)CD are largely unknown. Our aim was to identify causative genes for these disorders by genome-wide homozygosity mapping. We investigated 75 ACHM, 97 arCD, and 20 early-onset arCD probands and excluded the involvement of known genes for ACHM and arCD. Subsequently, we performed high-resolution SNP analysis and identified large homozygous regions spanning the *PDE6C* gene in one sibling pair with early-onset arCD and one sibling pair with incomplete ACHM. The *PDE6C* gene encodes the cone α subunit of cyclic guanosine monophosphate (cGMP) phosphodiesterase, which converts cGMP to 5′-GMP, and thereby plays an essential role in cone phototransduction. Sequence analysis of the coding region of *PDE6C* revealed homozygous missense mutations (p.R29W, p.Y323N) in both sibling pairs. Sequence analysis of 104 probands with arCD and 10 probands with ACHM revealed compound heterozygous *PDE6C* mutations in three complete ACHM patients from two families. One patient had a frameshift mutation and a splice defect; the other two had a splice defect and a missense variant (p.M455V). Cross-sectional retinal imaging via optical coherence tomography revealed a more pronounced absence of cone photoreceptors in patients with ACHM compared to patients with early-onset arCD. Our findings identify *PDE6C* as a gene for cone photoreceptor disorders and show that arCD and ACHM constitute genetically and clinically overlapping phenotypes.

Impairment or death of the cone photoreceptor cells is the clinical hallmark of cone disorders, which have an estimated prevalence of 1:30,000–1:40,000.[1,2] Achromatopsia (ACHM) (MIM *600827) is a stationary congenital autosomal recessive cone disorder characterized by low visual acuity (0.10–0.20 decimal Snellen equivalent), photophobia, nystagmus, and severe color vision defects. Patients with the complete ACHM subtype have no cone function on electroretinogram (ERG), whereas those with incomplete ACHM have residual cone function. Cone dystrophy (CD) (MIM *600827) is a progressive cone disorder in which patients may initially have normal cone function but develop progressive visual acuity loss, increasing photophobia, color vision disturbances, and diminished cone responses on ERG, usually in the first or second decade of life. The visual acuity of these patients generally worsens to legal blindness before the fourth decade of life.[3]

The genetic basis of these disorders has been partly elucidated during the last decade. Three genes have been implicated in ACHM: *CNGA3* (MIM *600053), *CNGB3* (MIM *605080), and *GNAT2* (MIM +139340). Mutations in these genes explain a majority of cases of this disease, but a fraction of cases still remain unsolved.[4–7] Several genes have been identified for the autosomal dominant[3,8,9] and X-linked forms of CD,[10,11] but little is known about the genetic causes of the most prevalent autosomal recessive (arCD) form. Four genes have been implicated in this form: *ABCA4* (MIM *601691),[12] *CACNA2D4* (MIM *608171),[13] *CNGB3* (MIM *605080),[14] and *KCNV2* (MIM *607604),[15,16] which together explain only ~10% of all cases.

We aimed to identify disease genes for cone photoreceptor disorders and investigated patients with ACHM and arCD. Patients were ascertained from various ophthalmic centers in the Netherlands, Belgium, the United Kingdom, and Canada. This study was approved by the local and national medical ethics committees and adhered to the tenets of the Declaration of Helsinki. All participants provided signed, informed consent for participation in the study, retrieval of medical records, and use of blood and DNA for research.

All available data on visual acuity, color vision, fundus appearance, and ERGs were retrieved from medical charts

[1]Department of Ophthalmology, Erasmus Medical Centre, PO Box 2040, 3000 CA Rotterdam, The Netherlands; [2]Department of Human Genetics, [3]Department of Ophthalmology, Radboud University Nijmegen Medical Centre, PO Box 9101, 6500 HB Nijmegen, The Netherlands; [4]Nijmegen Centre for Molecular Life Sciences, [5]Centre for Molecular and Biomolecular Informatics, Radboud University Nijmegen, PO Box 9102, 6500 HC Nijmegen, The Netherlands; [6]Centre for Medical Genetics, Ghent University Hospital, B-9000 Ghent, Belgium; [7]McGill Ocular Genetics Laboratory, McGill University Health Centre, Montreal, QC H3H 1P3, Canada; [8]Department of Ophthalmogenetics, Netherlands Institute for Neuroscience, 1105 BA Amsterdam, The Netherlands; [9]Institute of Human Genetics, Helmholtz Zentrum München, German Research Center for Environmental Health, D-85764 Neuherberg, Germany; [10]Division of Clinical Neurosciences, University of Southampton, Southampton SO16 6YD, UK; [11]Sensis Grave, 5361 HK Grave, The Netherlands; [12]Department of Ophthalmology, Ghent University Hospital, B-9000 Ghent, Belgium; [13]The Rotterdam Eye Hospital, PO Box 7000, 3000 LM Rotterdam, The Netherlands; [14]Department of Epidemiology, Erasmus Medical Centre, PO Box 2040, 3000 CA Rotterdam, The Netherlands
*Correspondence: f.cremers@antrg.umcn.nl
DOI 10.1016/j.ajhg.2009.06.016.

and updated by additional examinations including optical coherence tomography (OCT) and fundus photography. Recent ERGs were performed according to the recommendations of the International Society for Clinical Electrophysiology of Vision.[17] Patients could be stratified into three clinical categories: ACHM (n = 75 probands), arCD (n = 97 probands), and a group who had clear documentation of progressive cone dysfunction but already had impaired visual acuity in early childhood (early-onset arCD; n = 20 probands). We tested for the presence of known *ABCA4* mutations in all probands (A.A.H.J.T., unpublished data) and for the presence of *CNGB3* variants in all probands via sequence analysis.[5,7] When *CNGB3* variants were absent, all ACHM patients were analyzed for *CNGA3* and *GNAT2* variants via sequence analysis.[5,7] Finally, most of the arCD patients were analyzed for *KCNV2* variants via sequence analysis (A.A.H.J.T., unpublished data). These studies resulted in 116 probands—i.e., 11 ACHM, 85 arCD, and 20 early-onset arCD—with unknown etiology who formed the basis of the present genetic analyses.

We performed high-resolution SNP analysis (Affymetrix GeneChip Genome-Wide Human Array 5.0) on a subset of 76 patients from 64 families with autosomal recessive cone dysfunction from whom DNA was available. In 8 of these 64 families, the parents were consanguineous. Genotyping was performed with Genotype Console software (Affymetrix), and regions of homozygosity were calculated with Partek Genomics Solution software. Large identity by descent (IBD) regions (i.e., >5 Mb) were found in all consanguineous families and in 34 of the nonconsanguineous probands. In these 34 nonconsanguineous patients, we found a total of 57 IBD regions larger than 5 Mb, with an average size of 9 Mb (range 5–31 Mb).

In a sibling pair from a consanguineous marriage (family B) and in a sibling pair from a nonconsanguineous family (family A), we identified large homozygous regions on chromosome 10 (11 Mb and 26 Mb, respectively) (Figure 1A). The common 26 Mb homozygous region in the sibs from family A was the largest homozygous region (SNP boundaries SNP_A-2260521 and SNP_A-1892358); the second, third, and fourth largest regions measured 8, 4.3, and 4.2 Mb. The overlapping 11 Mb homozygous region in the affected sibs of family B was the second largest homozygous region (SNP boundaries SNP_A-2003359 and SNP_A-1804692). The largest region in this family spanned 25 Mb; the third and fourth largest regions measured 10 and 6 Mb. The overlapping homozygous region in both families spanned the *PDE6C* gene but no other obvious candidate genes (Figure 1A; see also Table S1 available online). These regions were not found in other patients.

PDE6C encodes the cone α subunit of cyclic guanosine monophosphate (cGMP) phosphodiesterase, an enzyme consisting of two α and two γ subunits that is essential in the cone phototransduction cascade. It converts the second messenger cGMP to 5′-GMP during light exposure. This results in closure of the cGMP-gated ion channel in the cone outer segment membrane, leading to hyperpolarization of the cell.[18]

Because *PDE6C* appeared to be an excellent candidate for cone photoreceptor disorders, we performed direct sequencing of all 22 exons (Figure 1B). We detected homozygous missense mutations in exon 1 in both sibling pairs of family A (Figures 1B–1D). The first proband (AII-1) and his brother (AII-2) carried a homozygous missense mutation (p.R29W) affecting a conserved residue just upstream of the first GAF (GAF-A) domain (acronym derived from proteins in which these domains were initially identified) (Figure 1B). The arginine residue at position 29 is fully conserved in all depicted orthologs of the cone and rod α subunits (PDE6C and PDE6A), except for in bovine and canine PDE6C (Figure 1E). The second proband (BII-1) and her brother (BII-2) carried the homozygous missense mutation p.Y323N (Figures 1C and 1D). This mutation affects a fully conserved residue located in the second GAF (GAF-B) domain (Figures 1B and 1E, mutation M4), a region of the protein that binds cGMP and regulates the activity of the enzyme.[19] Protein homology modeling of the GAF-B domain on the basis of a recent GAF-A crystal structure[19] shows that the p.Y323N mutation is located near the cGMP binding site. Although not directly interacting with cGMP, Y323 neighbors D322, which is in direct contact with bound cGMP, as shown in Figure 2. D322 tightly interacts with cGMP by means of two hydrogen bonds, one originating from the peptide main chain and one originating from the aspartic acid side chain. Mutation of Y323 to N is likely to alter the local backbone conformation and mobility and is also likely to affect D322 and its interaction with cGMP. Both the orientation and the mobility of the amino acids equivalent to D322 in other GAF domains have been suggested to be of crucial importance in determining affinity and selectivity of these domains for cGMP.[19] We hypothesize that the p.Y323N mutation will probably alter the affinity of cGMP for the regulatory GAF-B domain.

Subsequently, we analyzed the remaining patients (n = 114) for additional mutations in the *PDE6C* gene by direct sequencing of the coding region. Compound heterozygous mutations were detected in two additional probands. Patient CII-1 was compound heterozygous for a frameshift mutation (c.257_258 dupAG; p.L87GfsX57) in exon 1 and a 5 bp deletion (c.2367+1delGTAAG), which removes the first five nucleotides of intron 20, including the splice donor site (Figures 1C and 1D). An alternative splice donor site is predicted at position 2366 (splice prediction score 0.80, BGDP Splice Site Prediction by Neural Network).[20] Use of this splice site would lead to a shift in the open reading frame and premature termination of the phosphodiesterase 6C protein (p.E790SfsX12). Patient DII-1 and her affected sister (DII-2) revealed two missense variants (c.633G→C [p.E211D] and c.1363A→G [p.M455V]) (Figure 1C). The glutamic acid at position 211 is changed to the functionally conserved aspartic acid in five of six

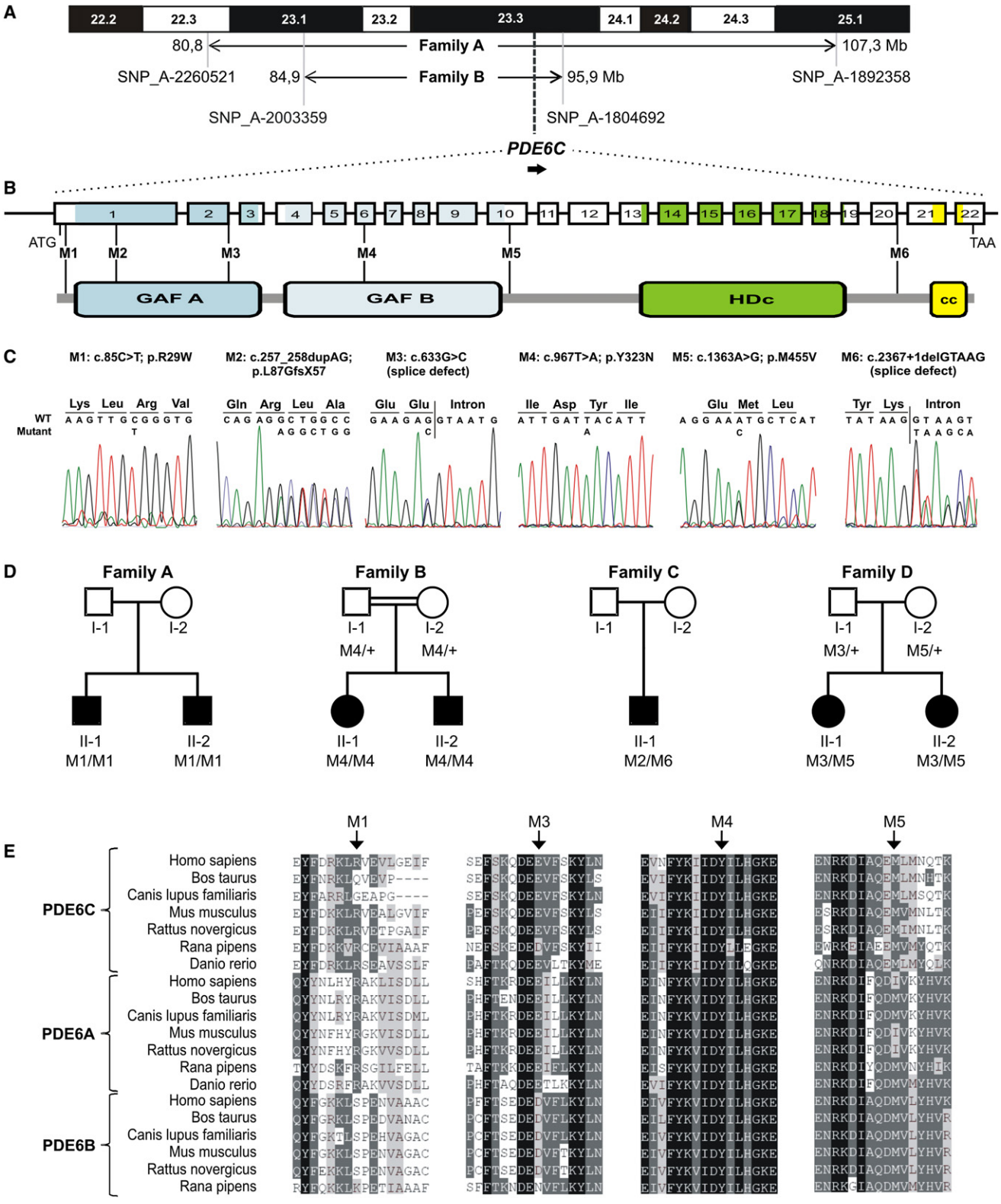

Figure 1. Molecular Genetic Characterization of the *PDE6C* Gene in Four Families with Autosomal Recessive Cone Photoreceptor Disorders

(A) The 10q22-q25 region and the homozygous regions identified in patients of families A and B. The SNPs flanking the homozygous regions and their genomic positions, from the March 2006 UCSC genome build (hg18), are indicated.

(B) Protein and genomic structure of PDE6C. GAF, acronym derived from proteins in which these domains were initially identified (cGMP-regulated mammalian phosphodiesterases, cyanobacterial adenylyl cyclases, and a formate-hydrogen lyase transcriptional activator); HDc, domain with highly conserved histidines (H) and aspartic acids (D); cc, coiled-coil domain. The six mutations are labeled M1 through M6.

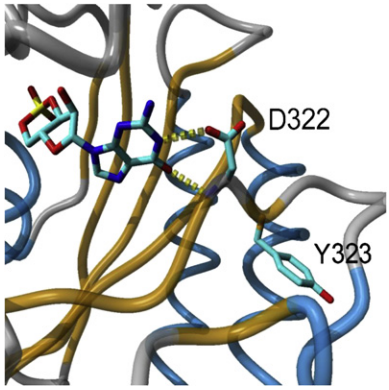

Figure 2. Molecular Modeling of Y323 in the GAF-B Domain of PDE6C
The individual side-chain orientations of D322 and Y323 are shown in magenta. A peptide backbone trace of the remainder of the model is shown, with β sheets colored orange and α helices colored blue. The mutation site Y323 is located adjacent to D322. The latter amino acid is shown interacting with bound cGMP via two hydrogen bonds, one originating from the peptide main chain and one originating from the aspartic acid side chain. Hydrogen bonds are indicated by yellow dashed lines.

homologous rod PDE β subunits, and in frog PDE6C, strongly suggesting that the predicted amino acid change is a functionally neutral variant. The c.633G→C variant does, however, affect the last nucleotide of exon 2 and is predicted to completely abolish the splice donor site (BGDP Splice Site Prediction by Neural Network).[20] Because no alternative splice donor sites are predicted, the mutation may result either in removal of exon 2 from the mRNA or in nonsplicing of intron 2 (106 bp). In both options, this would result in a disruption of the open reading frame. The p.M455V mutation affects a conserved residue located just downstream of the GAF-B domain (Figures 1B and 1E). In those families in which DNA was available from parents (families B and D), mutations M3, M4, and M5 segregated as expected for pathologic variants (Figure 1D). None of the six *PDE6C* mutations were found in 180 ethnically matched controls.

In four other unrelated patients with arCD, we found four different heterozygous amino acid changes (c.413T→C [p.L138S], c.696G→A [p.M232I], c.2096A→G [p.E699G], and c.2477T→C [p.I826T]). In these patients, we did not find a second mutation on the other allele in the coding region of this gene, despite complete *PDE6C* sequencing. We considered the possibility of a digenic disease model, with mutations in both *PDE6C* and an interacting gene, and performed sequence analysis of the gene encoding the cone γ subunit of cGMP phosphodiesterase (*PDE6H*). We did not detect mutations in this gene. The four heterozygous variants in *PDE6C* were not detected in 180 ethnically matched control individuals. The missense variants p.M232I, p.E699A, and p.I826T were predicted by SIFT software to be tolerated; only variant p.L138S was predicted not to be tolerated. Moreover, the isoleucine at position 826 is substituted by a threonine in the mouse and rat orthologs, rendering this a very likely benign amino acid change. The patients carrying the p.L138S, p.E699A, and p.I826T variants were part of the 5.0 Affymetrix SNP screening. A copy-number variant analysis of the SNP data with Partek GS software did not reveal a deletion or duplication of twenty intragenic SNPs and five copy-number variant probes evenly spaced across the *PDE6C* gene (Figure S1). Though very small deletions encompassing single exons or part of the promoter cannot be excluded, these data strongly suggest that the heterozygous *PDE6C* missense variants represent rare benign sequence variants.

Table 1 shows a summary of the clinical findings of all patients with *PDE6C* mutations on both alleles. Patients AII-1 and AII-2 carried a homozygous missense mutation, located just upstream of the GAF-A domain (Figure 1A). They showed an early-onset CD; their visual acuity and cone ERG progressively declined in their early teens. Patients BII-1 and BII-2 had a homozygous missense mutation in the GAF-B domain, which presumably affects the interaction with cGMP. This sibling pair presented with an incomplete ACHM; the cone ERG responses were significantly reduced but measurable both in childhood and on recent examination, whereas the rod ERG parameters were normal. Patient CII-1, carrying a protein-truncating mutation and a splice defect, had the most severe cone phenotype. At 4 years of age, the visual acuity was 0.10, the cone ERG was nonrecordable, and the rod function was completely normal (Figure 3). Patients DII-1 and DII-2, each carrying a splice defect and a p.M455V missense

(C) Chromatograms showing the *PDE6C* mutations.
(D) Pedigrees of early-onset cone dystrophy (family A), incomplete achromatopsia (family B), and complete achromatopsia (families C and D) and segregation analysis of the respective *PDE6C* variants. The parents in family A are not related to each other in the last three generations. BI-1 and BI-2 are first cousins.
(E) Evolutionary conservation of the altered amino acid residues in three families. PDE6A and PDE6C are rod and cone α subunits respectively; PDE6B is the rod β subunit. Using the Swiss-Prot database, we searched for their orthologs in as many species as possible and included, with the exception of *Danio rerio*, those present in all species. White lettered residues on a black background are fully conserved between different species in all three subunits. White lettered residues on a gray background are conserved in most sequences. Black lettered residues with light gray background are similar to amino acid residues in other orthologs and homologs. The arginine residue at position 29 is fully conserved in all orthologs of both α subunits (PDE6C and PDE6A), except for bovine and canine PDE6C. The aspartic acid residue in the GAF-A domain at position 211 is conserved or replaced by a functionally conserved glutamic acid residue in 19 of 20 orthologs and homologs. This observation strongly suggests that the predicted p.E211D substitution in family D is neutral and that the effect of c.633G→C on the splice site is pathologic. The tyrosine residue located in the GAF-B domain at position 323 is completely conserved among all three PDE6 subunits. The methionine residue at position 455 is conserved or substituted by a functionally conserved isoleucine in all PDE6 molecules.

Table 1. Clinical Findings in Probands and Affected Relatives, Stratified According to Genotype

Patient	*PDE6C* Mutations	Diagnosis	Age First Exam	Age Last Exam	BVCA Best Eye		Visual Complaints		Refractive Error Spherical Equivalent	Color Vision Defects		Macular Appearance		Periphery Last Exam	Cone ERG	
					First Exam	Last Exam	Photophobia	Nystagmus		First Exam	Last Exam	First Exam	Last Exam		First Exam	Last Exam
AII-1	p.R29W/ p.R29W	Early-onset CD	6	51	0.40	0.16	Yes	Yes	−11	Severe	Severe	No foveal reflex	Mild pigmentary changes	Normal	Reduced	No responses
AII-2	p.R29W/ p.R29W	Early-onset CD	7	47	0.30	0.20	Yes	Yes	−3.5	Severe	Severe	Pigmentary changes	Pigmentary changes	Normal	Reduced	No responses
BII-1	p.Y323N/ p.Y323N	Incomplete ACHM	7	23	0.16	0.10	No	Yes	−10	Severe	Severe	Mild pigmentary changes	Mild pigmentary changes	Normal	ND	ND
BII-2	p.Y323N/ p.Y323N	Incomplete ACHM	10	20	0.16	0.10	No	Yes	−2	Severe	Severe	No foveal reflex	No foveal reflex	Normal	Reduced	Reduced
CII-1	p.L87GfsX57/ c.2367+1 delGTAAG	Complete ACHM	2	4	0.10	0.10	Severe	Yes	+10.5	Severe	Severe	No foveal reflex	No foveal reflex	Normal	No responses	No responses
DII-1	c.633G→C/ p.M455V	Complete ACHM	12	37	0.16	0.10	Severe	Yes	−5	Severe	Severe	No foveal reflex	Mild pigmentary changes	Normal	No responses	No responses
DII-2	c.633G→C/ p.M455V	Complete ACHM	11	36	0.16	0.10	Severe	Yes	−1.5	Severe	Severe	No foveal reflex	No foveal reflex	Normal	No responses	No responses

Abbreviations are as follows: BVCA, best corrected visual acuity; CD, cone dystrophy; ACHM, achromatopsia; ND, not determined.

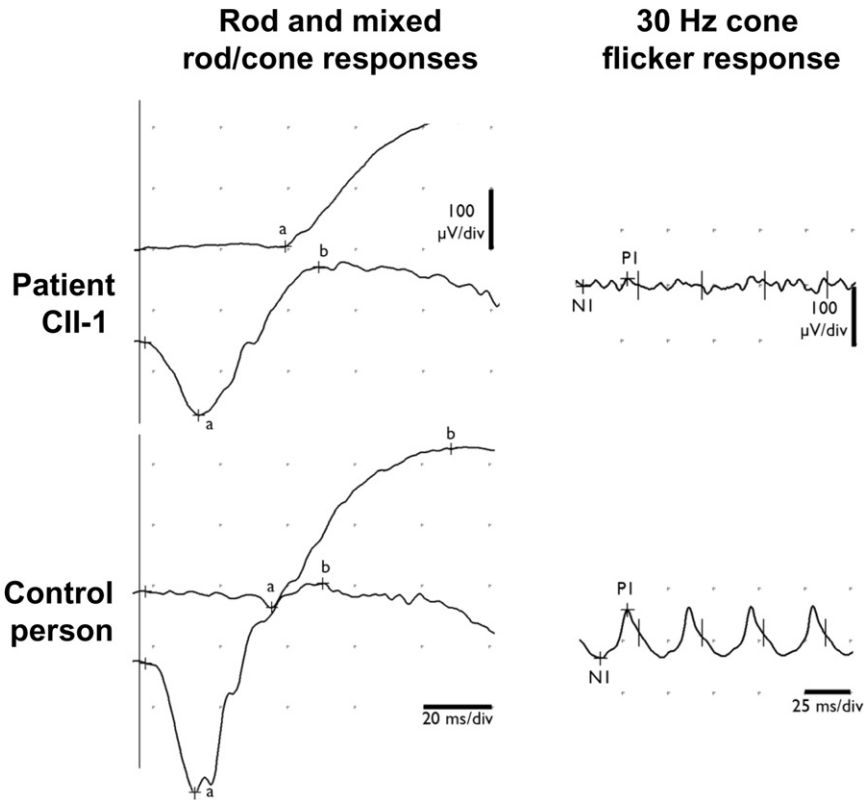

Figure 3. Electroretinogram of Patient CII-1

An electroretinogram performed with an abbreviated standard International Society for Clinical Electrophysiology of Vision protocol at the age of 4 years without sedation is shown at top, with normal control traces at bottom for purposes of comparison. Note normal rod-specific response (top trace at left), with no significant contribution of cones to combined rod-cone response (bottom trace at left for patient CII-1); dark-adapted oscillatory responses as seen on ascending limb of the b-wave are residual at most. The absence of cone-specific function was demonstrated by the absence of cone-specific response to 30 Hz flicker stimulation (at right).

mutation, were clinically diagnosed as complete ACHM because they exhibited a low visual acuity of 0.16 with nystagmus since early childhood and absent cone responses on ERG.

In the adult patients, we performed Heidelberg Spectralis OCT at the most recent ophthalmologic examination. The absence of the photoreceptor cell layer in the fovea, a site with predominantly cone photoreceptor cells, was apparent in all patients. A typical OCT picture for patients from family A (patient AII-2) is shown in Figure 4B; a characteristic OCT image for patients from families B and D (patient DII-1) is shown in Figure 4D. The area of absent cone photoreceptors in patient DII-1, which spans almost the entire fovea, is significantly larger than the lesion in patient AII-2 (Figures 4B and 4D). We hypothesize that the missense variant in family A, which is located outside functionally important domains, may have a less severe effect on the function of PDE6C than the mutations observed in the other families.

In zebrafish, mutations in the ortholog of *PDE6C* are responsible for progressive cone photoreceptor degeneration.[21,22] An intron 11 splice acceptor site mutation[21] and a p.M175R missense mutation in the GAF-A domain[22] lead to rapid degeneration of cone photoreceptors soon after their formation. Unlike in humans, zebrafish photoreceptors are continuously generated at the retinal margin by a population of mitotic progenitor cells, so cone photoreceptors can be found at the periphery throughout the life of these mutant fish. The splice site mutation in zebrafish also results in the degeneration of rod photoreceptors in the central part of the retina.[21] In zebrafish with the p.M175R missense mutation, rods show an abnormal morphology and rhodopsin mislocalization but otherwise function normally.[22] These findings suggest that the effect of the zebrafish *Pde6c* p.M175R mutation is more cone-specific than that of the *Pde6c* splice defect.

To test the involvement of rod photoreceptors in human patients, we repeated the ERG on the two oldest patients with *PDE6C* mutations (AII-1 and AII-2; 47 and 51 years old, respectively), and we did not find abnormal rod responses. Normal rod responses were also observed in patients CII-1, DII-1, and DII-2. We concluded that rod involvement does not appear to be a major consequence of *PDE6C* mutations in humans, although some dysfunction of rods may still occur later in life.

In conclusion, through homozygosity mapping of patients with cone photoreceptor disorders from nonconsanguineous and consanguineous families, we identified another causative gene, *PDE6C*. PDE6C has a crucial role in the cone phototransduction cascade. Similar to the other disease genes in this cascade (*CNGA3*, *CNGB*, and *GNAT2*),[4–6] *PDE6C* mutations result in a severe early-onset cone disorder. We show that early-onset CD, incomplete ACHM, and complete ACHM form a continuous spectrum of a similar etiology. The observed variability in phenotypes may be a result of differences in the functional effects of *PDE6C* mutations. Our findings will improve diagnosis and counseling of patients and their families and represent another step toward solving the etiology of cone photoreceptor disorders.

Supplemental Data

Supplemental Data include one table and one figure and can be found with this article online at http://www.ajhg.org/.

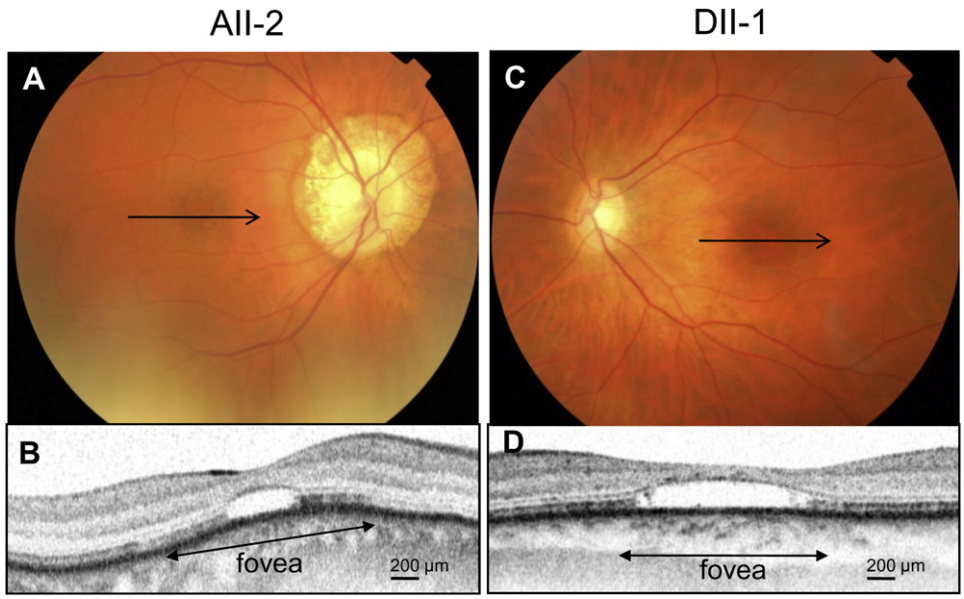

Figure 4. Retinal Phenotypes of Early-Onset Cone Dystrophy and Complete Achromatopsia in Families A and D
(A) Fundus photography of the right eye of patient AII-2, performed at age 51 years, showing myopic changes in the peripapillary region. In the macular region, mild pigmentary changes are present. The arrow denotes the position of the optical coherence tomography (OCT) image in (B).
(B) The Heidelberg Spectralis OCT of this patient reveals a serous detachment of the photoreceptor layer in the central fovea. The retinal pigment epithelium is intact, but the outer and inner segments of the photoreceptors are absent. The length of the lesion is ~500 μm. The OCT cross-section is not fully perpendicular.
(C) Fundus photography of the left eye of patient DII-1, performed at age 37 years, showing mild pigmentary changes in the macula. The arrow denotes the position of the OCT image in (D).
(D) The Heidelberg Spectralis OCT of this patient displays a large area of ~1300 μm with absent cone photoreceptors, which involves almost the entire fovea.

Acknowledgments

We thank R. Bernaerts-Biskop for extensive assistance with data collection and V. Somervuo for performance of OCTs. We thank S. van der Velde-Visser and C. Beumer for expert technical assistance. This study was financially supported by Prof. Dr. Henkes Stichting, Nijmeegse Oogonderzoek Stichting, Stichting Wetenschappelijk Onderzoek Oogziekenhuis (SWOO), the Rotterdam Eye Hospital, Macula Degeneratie Fonds (MD Fonds), Algemene Nederlandse Vereniging ter Voorkoming van Blindheid (ANVVB), Dr. F.P. Fischer Stichting, Gelderse Blinden Stichting, Landelijke Stichting voor Blinden en Slechtzienden (LSBS), Stichting Blindenhulp, Stichting Blinden-penning, Stichting Nederlands Oogheelkundig Onderzoek (SNOO), Stichting Ondersteuning Oogheelkunde's-Gravenhage (OOG), Stichting ter Verbetering van het Lot der Blinden Nederland, Research Foundation Flanders (FWO) grant number G.0043.06N, Foundation Fighting Blindness–Canada, Fonds de la recherche en santé du Québec (FRSQ), and the Canadian Institutes of Health Research (CIHR).

Received: April 24, 2009
Revised: June 8, 2009
Accepted: June 24, 2009
Published online: July 16, 2009

Web Resources

The URLs for data presented herein are as follows:

Amino acid change prediction of pathogenicity, http://sift.jcvi.org
Mutation nomenclature, http://www.hgvs.org
Online Mendelian Inheritance in Man (OMIM), http://www.ncbi.nlm.nih.gov/Omim/
PDE6 ortholog search in UniProt Knowledgebase, http://www.expasy.ch/tools/blast/
Splice site prediction, http://www.fruitfly.org/seq_tools/splice.html
UCSC human genome database build hg18, March 2006, http://www.genome.ucsc.edu

References

1. Michaelides, M., Hunt, D.M., and Moore, A.T. (2004). The cone dysfunction syndromes. Br. J. Ophthalmol. *88*, 291–297.
2. Hamel, C.P. (2007). Cone rod dystrophies. Orphanet J. Rare Dis. *2*, 1–7.
3. Michaelides, M., Hardcastle, A.J., Hunt, D.M., and Moore, A.T. (2006). Progressive cone and cone-rod dystrophies: Phenotypes and underlying molecular genetic basis. Surv. Ophthalmol. *51*, 232–258.
4. Kohl, S., Baumann, B., Rosenberg, T., Kellner, U., Lorenz, B., Vadala, M., Jacobson, S.G., and Wissinger, B. (2002). Mutations in the cone photoreceptor G-protein alpha-subunit gene GNAT2 in patients with achromatopsia. Am. J. Hum. Genet. *71*, 422–425.
5. Kohl, S., Varsanyi, B., Antunes, G.A., Baumann, B., Hoyng, C.B., Jagle, H., Rosenberg, T., Kellner, U., Lorenz, B., Salati, R., et al. (2005). CNGB3 mutations account for 50% of all cases with autosomal recessive achromatopsia. Eur. J. Hum. Genet. *13*, 302–308.

6. Wissinger, B., Gamer, D., Jagle, H., Giorda, R., Marx, T., Mayer, S., Tippmann, S., Broghammer, M., Jurklies, B., Rosenberg, T., et al. (2001). CNGA3 mutations in hereditary cone photoreceptor disorders. Am. J. Hum. Genet. *69*, 722–737.
7. Thiadens, A.A.H.J., Slingerland, N.W.R., Roosing, S., van Schooneveld, M.J., van Lith-Verhoeven, J.J.C., van Moll-Ramirez, N., van den Born, L.I., Hoyng, C.B., Cremers, F.P.M., and Klaver, C.C.W. (2009). Genetic etiology and clinical consequences of complete and incomplete achromatopsia. Ophthalmology, in press.
8. Jiang, L., Katz, B.J., Yang, Z., Zhao, Y., Faulkner, N., Hu, J., Baird, J., Baehr, W., Creel, D.J., and Zhang, K. (2005). Autosomal dominant cone dystrophy caused by a novel mutation in the GCAP1 gene (GUCA1A). Mol. Vis. *11*, 143–151.
9. Nishiguchi, K.M., Sokal, I., Yang, L., Roychowdhury, N., Palczewski, K., Berson, E.L., Dryja, T.P., and Baehr, W. (2004). A novel mutation (I143NT) in guanylate cyclase-activating protein 1 (GCAP1) associated with autosomal dominant cone degeneration. Invest. Ophthalmol. Vis. Sci. *45*, 3863–3870.
10. Vervoort, R., Lennon, A., Bird, A.C., Tulloch, B., Axton, R., Miano, M.G., Meindl, A., Meitinger, T., Ciccodicola, A., and Wright, A.F. (2000). Mutational hot spot within a new RPGR exon in X-linked retinitis pigmentosa. Nat. Genet. *25*, 462–466.
11. Demirci, F.Y., Rigatti, B.W., Wen, G., Radak, A.L., Mah, T.S., Baic, C.L., Traboulsi, E.I., Alitalo, T., Ramser, J., and Gorin, M.B. (2002). X-linked cone-rod dystrophy (locus COD1): Identification of mutations in RPGR exon ORF15. Am. J. Hum. Genet. *70*, 1049–1053.
12. Kitiratschky, V.B., Grau, T., Bernd, A., Zrenner, E., Jagle, H., Renner, A.B., Kellner, U., Rudolph, G., Jacobson, S.G., Cideciyan, A.V., et al. (2008). ABCA4 gene analysis in patients with autosomal recessive cone and cone rod dystrophies. Eur. J. Hum. Genet. *16*, 812–819.
13. Wycisk, K.A., Zeitz, C., Feil, S., Wittmer, M., Forster, U., Neidhardt, J., Wissinger, B., Zrenner, E., Wilke, R., Kohl, S., et al. (2006). Mutation in the auxiliary calcium-channel subunit CACNA2D4 causes autosomal recessive cone dystrophy. Am. J. Hum. Genet. *79*, 973–977.
14. Michaelides, M., Aligianis, I.A., Ainsworth, J.R., Good, P., Mollon, J.D., Maher, E.R., Moore, A.T., and Hunt, D.M. (2004). Progressive cone dystrophy associated with mutation in CNGB3. Invest. Ophthalmol. Vis. Sci. *45*, 1975–1982.
15. Thiagalingam, S., McGee, T.L., Weleber, R.G., Sandberg, M.A., Trzupek, K.M., Berson, E.L., and Dryja, T.P. (2007). Novel mutations in the KCNV2 gene in patients with cone dystrophy and a supernormal rod electroretinogram. Ophthalmic Genet. *28*, 135–142.
16. Wissinger, B., Dangel, S., Jagle, H., Hansen, L., Baumann, B., Rudolph, G., Wolf, C., Bonin, M., Koeppen, K., Ladewig, T., et al. (2008). Cone dystrophy with supernormal rod response is strictly associated with mutations in KCNV2. Invest. Ophthalmol. Vis. Sci. *49*, 751–757.
17. Marmor, M.F., Fulton, A.B., Holder, G.E., Miyake, Y., Brigell, M., and Bach, M. (2009). ISCEV Standard for full-field clinical electroretinography (2008 update). Doc. Ophthalmol. *118*, 69–77.
18. Burns, M.E., and Baylor, D.A. (2001). Activation, deactivation, and adaptation in vertebrate photoreceptor cells. Annu. Rev. Neurosci. *24*, 779–805.
19. Martinez, S.E., Heikaus, C.C., Klevit, R.E., and Beavo, J.A. (2008). The structure of the GAF A domain from phosphodiesterase 6C reveals determinants of cGMP binding, a conserved binding surface, and a large cGMP-dependent conformational change. J. Biol. Chem. *283*, 25913–25919.
20. Reese, M.G., Eeckman, F.H., Kulp, D., and Haussler, D. (1997). Improved splice site detection in Genie. J. Comput. Biol. *4*, 311–323.
21. Stearns, G., Evangelista, M., Fadool, J.M., and Brockerhoff, S.E. (2007). A mutation in the cone-specific pde6 gene causes rapid cone photoreceptor degeneration in zebrafish. J. Neurosci. *27*, 13866–13874.
22. Nishiwaki, Y., Komori, A., Sagara, H., Suzuki, E., Manabe, T., Hosoya, T., Nojima, Y., Wada, H., Tanaka, H., Okamoto, H., et al. (2008). Mutation of cGMP phosphodiesterase 6alpha'-subunit gene causes progressive degeneration of cone photoreceptors in zebrafish. Mech. Dev. *125*, 932–946.